

Distributed MAC Protocol Design for Full-Duplex Cognitive Radio Networks

Le Thanh Tan and Long Bao Le

Abstract—In this paper, we consider the Medium Access Control (MAC) protocol design for full-duplex cognitive radio networks (FDCRNs). Our design exploits the fact that full-duplex (FD) secondary users (SUs) can perform spectrum sensing and access simultaneously, which enable them to detect the primary users' (PUs) activity during transmission. The developed FD MAC protocol employs the standard backoff mechanism as in the 802.11 MAC protocol. However, we propose to adopt the frame fragmentation during the data transmission phase for timely detection of active PUs where each data packet is divided into multiple fragments and the active SU makes sensing detection at the end of each data fragment. Then, we develop a mathematical model to analyze the throughput performance of the proposed FD MAC protocol. Furthermore, we propose an algorithm to configure the MAC protocol so that efficient self-interference management and sensing overhead control can be achieved. Finally, numerical results are presented to evaluate the performance of our design and demonstrate the throughput enhancement compared to the existing half-duplex (HD) cognitive MAC protocol.

Index Terms—MAC protocol, spectrum sensing, optimal sensing, throughput maximization, full-duplex cognitive radios.

I. INTRODUCTION

Engineering MAC protocols for efficient sharing of white spaces is an important research problem for cognitive radio networks (CRNs). In general, a cognitive MAC protocol must realize both the spectrum sensing and access functions so that timely detection of the PUs' activity and effective spectrum sharing among different SUs can be achieved. Most existing research works on cognitive MAC protocols have focused on the design and analysis of half-duplex CRNs (e.g., see [1], [2] and references therein). Due to the half-duplex constraint, SUs typically employ the two-stage sensing/access procedure where they sense the spectrum in the first stage before accessing available channels for data transmission in the second stage [3] – [6]. These HD MAC protocols may not exploit the white spaces very efficiently since significant sensing time can be required, which would otherwise be utilized for data transmission. Moreover, SUs may not timely detect the PUs' activity during data transmission, which causes severe interference to active PUs.

Thanks to recent advances in the full-duplex technologies, some recent works propose more efficient full-duplex (FD) spectrum access design for cognitive radio networks [7] where each SU can perform sensing and transmission simultaneously [8]. In general, the self-interference¹ due to simultaneous sensing and access may lead to degradation on the SUs' spectrum sensing performance. In [7], the authors consider the cognitive FD MAC design where they assume that SUs

perform sensing in multiple small time slots to detect the PU's activity during transmission, which may not be efficient. Moreover, they assume that the PU can change its idle/busy status at most once during the SU's transmission, which may not hold true if the SU's data packets are long. Our FD cognitive MAC design overcomes these limitations where we propose to employ frame fragmentation with appropriate sensing design for timely protection of the PU and we optimize the sensing duration to maximize the network throughput.

Specifically, our FD MAC design employs the standard backoff mechanism as in the 802.11 MAC protocol to solve contention among SUs for compatibility. However, the winning SU of the contention process performs simultaneous sensing and transmission during the access phase where each data packet is divided into multiple data fragments and sensing decisions are taken at the end of individual data fragments. This packet fragmentation enables timely detection of PUs since the data fragment time is chosen to be smaller than the required channel evacuation time. We then develop a mathematical model for throughput performance analysis of the proposed FD MAC design considering the imperfect sensing effect. Moreover, we propose an algorithm to configure different design parameters including data fragment time, SU's transmit power, and the contention window to achieve the maximum throughput. Finally, we present numerical results to illustrate the impacts of different protocol parameters on the throughput performance and the throughput enhancement compared to the existing HD MAC protocol.

II. SYSTEM AND PU ACTIVITY MODELS

A. System Model

We consider a network setting where n_0 pairs of SUs opportunistically exploit white spaces on a frequency band for data transmission. We assume that each SU is equipped with one full-duplex transceiver, which can perform sensing and transmission simultaneously. However, SUs suffer from self-interference from its transmission during sensing (i.e., transmitted signals are leaked into the received PU signal). We denote I as the average self-interference power where it can be modeled as $I = \zeta (P_s)^\xi$ [8] where P_s is the SU transmit power, ζ and ξ ($0 \leq \xi \leq 1$) are some predetermined coefficients which capture the self-interference cancellation quality. We design a asynchronous MAC protocol where no synchronization is assumed between SUs and PUs. We assume that different pairs of SUs can overhear transmissions from the others (i.e., collocated networks). In the following, we refer to pair i of SUs as secondary link i or flow i interchangeably.

B. Primary User Activity

We assume that the PU's idle/busy status follows two independent and identical distribution processes. Here the

¹The authors are with INRS-EMT, University of Quebec, Montréal, Québec, Canada. Emails: {lethanh,long.le}@emt.inrs.ca.

¹Self-interference is due to the power leakage from the transmitter to the receiver of a full-duplex transceiver.

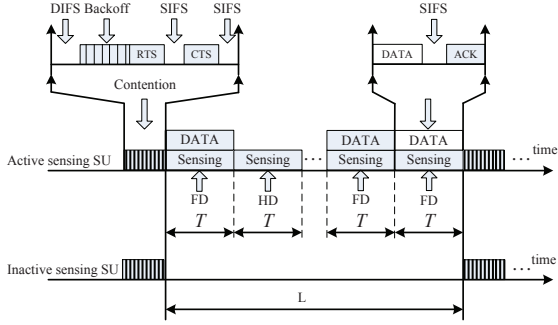


Fig. 1. Timing diagram of the proposed full-duplex MAC protocol.

channel is available and busy for the secondary access if the PU is in the idle and busy states, respectively. Let \mathcal{H}_0 and \mathcal{H}_1 denote the events that the PU is idle and active, respectively. To protect the PU, we assume that SUs must stop their transmission and evacuate from the channel within the maximum delay of T_{eva} , which is referred to as channel evacuation time.

Let τ_{ac} and τ_{id} denote the random variables which represent the durations of channel active and idle states, respectively. We assume that τ_{ac} and τ_{id} are larger than T_{eva} . We denote probability density functions of τ_{ac} and τ_{id} as $f_{\tau_{\text{ac}}}(t)$ and $f_{\tau_{\text{id}}}(t)$, respectively. In addition, let $\mathcal{P}(\mathcal{H}_0) = \frac{\tau_{\text{id}}}{\tau_{\text{id}} + \tau_{\text{ac}}}$ and $\mathcal{P}(\mathcal{H}_1) = 1 - \mathcal{P}(\mathcal{H}_0)$ present the probabilities that the channel is available and busy, respectively.

III. MAC PROTOCOL DESIGN

For contention resolution, we assume that SUs employ the backoff as in the standard CSMA/CA protocol [9]. In particular, SU transmitters perform carrier sensing and start the backoff after the channel is sensed to be idle in an interval referred to as DIFS (DCF Interframe Space). Specifically, each SU chooses a random backoff time, which is uniformly distributed in the range $[0, 2^i W - 1]$, $0 \leq i \leq m$ and starts counting down while carrier sensing the channel where W denotes the minimum backoff window and m is the maximum backoff stage. For simplicity, we assume that $m=1$ in the throughput analysis in the next section and we refer to W simply as the contention window.

Let σ denote a mini-slot interval, each of which corresponds one unit of the backoff time counter. Upon hearing a transmission from other secondary links or PUs, all SUs will “freeze” its backoff time counter and reactivate when the channel is sensed idle again. Otherwise, if the backoff time counter reaches zero, the underlying secondary link wins the contention. To complete the reservation, the four-way handshake with Request-to-Send/Clear-to-Send (RTS/CTS) exchanges will be employed to reserve the available channel for transmission in the next stage. Specifically, the secondary transmitter sends RTS to the secondary receiver and waits until it successfully receives CTS from the secondary receiver before sending the data. All other SUs, which hear the RTS and CTS from the secondary winner, defer to access the channel for a duration equal to the data packet length, L . Furthermore, the standard small interval, namely SIFS (Short Interframe Space), is used before the transmissions of CTS, ACK and data frame as described in [9].

We assume that the data length of the SU transmitter, L ($L = \bar{K}T$) is larger than the evacuation time, T_{eva} . Hence, SUs

divide each packet into \bar{K} equal-size data fragments, each of which is transmitted in duration T . Moreover, T is chosen to be smaller than T_{eva} so that timely evacuation from the busy channel can be realized. In addition, the active SU transmitter simultaneously senses the PU activity and transmits its data in each fragment where it makes one sensing decision on the idle/active channel status at the end of each data fragment. Furthermore, if the sensing outcome at one particular fragment indicates an “available” channel then the active SU transmitter performs concurrent sensing and transmission in the next fragment (called full-duplex (FD) sensing); otherwise, it only performs sensing without transmission (referred to as half-duplex (HD) sensing). This design allows to protect the PU with evacuation delay at most T if the sensing is perfect. We assume that SU’s transmit power is set equal to P_s where we will optimize this parameter to achieve good tradeoff between self-interference mitigation and high communication rate later. The timing diagram of this proposed FD MAC protocol is illustrated in Fig. 1.

IV. THROUGHPUT ANALYSIS

We perform throughput analysis for the saturated system where all SUs are assumed to always have data to transmit [9]. Let $\mathcal{P}_{\text{succ}}(i_0)$ denote the probability that the SU successfully reserves the channel (i.e., the RTS and CTS are exchanged successfully), $T_{\text{ove}}(i_0)$ represent the time overhead due to backoff and RTS/CTS exchanges, and \mathcal{T}^{i_0} denote the average conditional throughput in bits/Hz for the case where the back-off counter of the winning SU is equal to i_0 ($i_0 \in [0, W - 1]$). Then, the normalized throughput can be written as

$$\mathcal{N}\mathcal{T} = \sum_{i_0=0}^{W-1} \mathcal{P}_{\text{succ}}(i_0) \times \frac{\mathcal{T}^{i_0}}{T_{\text{ove}}(i_0) + \bar{K}T}. \quad (1)$$

In this expression, we have considered all possible values of the backoff counter of the winning SU in $[0, W - 1]$. In what follows, we derive the quantities $\mathcal{P}_{\text{succ}}(i_0)$, $T_{\text{ove}}(i_0)$, and \mathcal{T}^{i_0} .

A. Derivations of $\mathcal{P}_{\text{succ}}(i_0)$ and $T_{\text{ove}}(i_0)$

The event that the SU successfully reserves the channel for the case the winning SU has its backoff counter equal to i_0 occurs if all other SUs choose their backoff counters larger than i_0 . So the probability of this event ($\mathcal{P}_{\text{succ}}(i_0)$) can be expressed as follows:

$$\mathcal{P}_{\text{succ}}(i_0) = n_0 \frac{1}{W} \left(\frac{W - 1 - i_0}{W} \right)^{n_0 - 1}. \quad (2)$$

Moreover, the corresponding overhead involved for successful channel reservation at backoff slot i_0 is

$$T_{\text{ove}}(i_0) = i_0 \times \sigma + 2SIFS + RTS + CTS + DIFS \quad (3)$$

where σ , $SIFS$, $DIFS$, RTS and CTS represent the duration of backoff slot, the durations of one SIFS, one DIFS, RTS , and CTS control packets, respectively.

B. Derivation of \mathcal{T}^{i_0}

The quantity \mathcal{T}^{i_0} can be derived by studying the transmission phase which spans \bar{K} data fragment intervals each with length T . Note that the PU’s activity is not synchronized with the SU’s transmission; therefore, the PU can change its

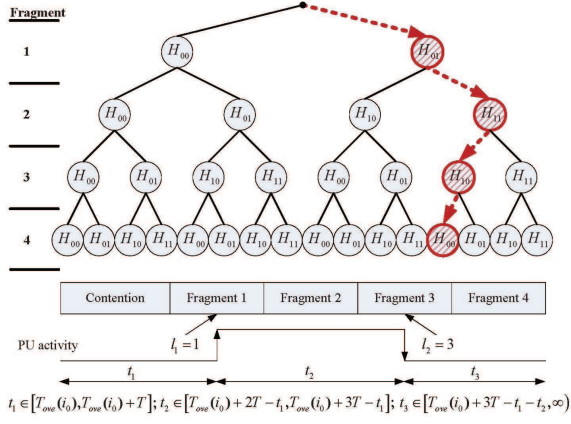


Fig. 2. PU's activity patterns.

active/idle status any time. It can be verified that there are four possible events related to the status changes of the PU during any particular data fragment, which are defined as follows. Let \mathcal{H}_{00} be the event that the PU is idle for the whole fragment interval; \mathcal{H}_{10} denote the event that PU is first active and then becomes idle by the end of the fragment; \mathcal{H}_{11} be the event that the PU is active for the whole fragment; and finally, \mathcal{H}_{01} capture the event that PU is first idle and then becomes active by the end of the fragment. Here, there can be at most one transition between the active and idle states during one fragment time. This holds because we have τ_{ac} and τ_{id} are larger than the fragment time T (since T_{eva} is larger than T ; τ_{ac} and τ_{id} are larger than T_{eva}).

The average throughput achieved by the secondary network depends on the PU's activity and sensing outcomes at every fragment. For any particular fragment, if the sensing outcome indicates an available channel then the winning SU will perform concurrent transmission and sensing in the next fragment (FD sensing); otherwise, it will perform sensing only in the next fragment (HD sensing) and hence the achievable throughput is zero. Moreover, the throughput and sensing outcome also depend on how the PU changes its state at one particular fragment.

In what follows, we present the steps to calculate \mathcal{T}^{i0} . We first generate all possible patterns capturing how the PU changes its idle/active status over all \bar{K} fragments. For each generated pattern, we then consider all possible sensing outcomes in all fragments. Moreover, we quantify the achieved throughput conditioned on individual cases with corresponding PU's statuses and sensing outcomes in all \bar{K} fragments based on which the overall average throughput can be calculated.

Let \mathcal{S}_i denote one particular pattern i capturing the corresponding changes of the PU's idle/active status and \mathcal{AS} denote the set of all possible patterns. There are $2^{\bar{K}}$ possible patterns since the PU either changes or maintains the status (idle or active status) in each fragment. Note that each pattern \mathcal{S}_i comprises a sequence of state changes represented by possible events \mathcal{H}_{ij} . For convenience, we define a pattern \mathcal{S}_i by the corresponding four sets \mathcal{S}_i^{00} , \mathcal{S}_i^{10} , \mathcal{S}_i^{01} , and \mathcal{S}_i^{11} whose elements are fragment indexes during which the channel state changes corresponding to \mathcal{H}_{00} , \mathcal{H}_{10} , \mathcal{H}_{01} and \mathcal{H}_{11} occur, respectively. For example, if one pattern has the PU's state changes as \mathcal{H}_{00} , \mathcal{H}_{01} , \mathcal{H}_{11} , \mathcal{H}_{11} in this order then we have $\mathcal{S}_i^{00} = \{1\}$, $\mathcal{S}_i^{10} = \emptyset$, $\mathcal{S}_i^{01} = \{2\}$, and $\mathcal{S}_i^{11} = \{3, 4\}$. Fig. 2

shows all possible patterns for $\bar{K} = 4$. Then, the conditional throughput \mathcal{T}^{i0} can be written as

$$\mathcal{T}^{i0} = \sum_{i=1}^{|\mathcal{AS}|} \mathcal{T}^{i0} \{\mathcal{S}_i\} \quad (4)$$

where $\mathcal{T}^{i0} \{\mathcal{S}_i\}$ is the throughput (bits/Hz) for the pattern \mathcal{S}_i .

Consider one particular pattern \mathcal{S}_i . Let Ω_i be the set with cardinality ρ_i whose elements are fragment indexes l_j^i in which the PU changes its state. Moreover, let Γ_i be another set also with cardinality ρ_i whose elements t_j^i are time intervals between consecutive PU's state changes. In the following, we omit index i in parameters l_j^i and t_j^i for brevity. We show one particular pattern \mathcal{S}_i with the parameter t_j in Fig. 2 (the corresponding \mathcal{S}_i is indicated by dash lines). For convenience, we denote $\int_{t=a}^b$ as $\int_{t \in \mathcal{R}}$ where $\mathcal{R} \equiv [a, b]$ is the range of t . Moreover, we define $\mathcal{R}_1 = [T_{ove}(i_0) + (l_1 - 1)T, T_{ove}(i_0) + l_1T]$ to be the range for t_1 . Similarly, the range for t_j is $\mathcal{R}_j = [T_{ove}(i_0) + (l_j - 1)T - \sum_{r=1}^{j-1} t_r, T_{ove}(i_0) + l_jT - \sum_{r=1}^{j-1} t_r]$; then the range for t_{ρ_i} can be also expressed as $\mathcal{R}_{\rho_i} = [T_{ove}(i_0) + (l_{\rho_i} - 1)T - \sum_{r=1}^{\rho_i-1} t_r, T_{ove}(i_0) + l_{\rho_i}T - \sum_{r=1}^{\rho_i-1} t_r]$; and finally the range for t_{ρ_i+1} is written as $\mathcal{R}_{\rho_i+1} = [T_{ove}(i_0) + \bar{K}T - \sum_{r=1}^{\rho_i} t_r, \infty)$.

Using these notations, $\mathcal{T}^{i0} \{\mathcal{S}_i\}$ can be written as

$$\mathcal{T}^{i0} \{\mathcal{S}_i\} = \mathcal{P}(\mathcal{H}_0) \int_{t_1 \in \mathcal{R}_1} \dots \int_{t_j \in \mathcal{R}_j} \dots \int_{t_{\rho_i} \in \mathcal{R}_{\rho_i}} \int_{t_{\rho_i+1} \in \mathcal{R}_{\rho_i+1}} \sum_{k=1}^{2^{\bar{K}}} \prod_{j_1 \in \Phi_k^0} \mathcal{P}_{j_1}(\vec{t}^k) \prod_{j_2 \in \Phi_k^1} \bar{\mathcal{P}}_{j_2}(\vec{t}^k) \sum_{j_3 \in \bar{\Phi}_k^0} T_{j_3}(\vec{t}^k) \quad (5)$$

$$f_{t_1}(t_1) \cdot f_{t_2}(t_2) \cdot \dots \cdot f_{t_{\rho_i}}(t_{\rho_i}) f_{t_{\rho_i+1}}(t_{\rho_i+1}) dt_1 \cdot \dots \cdot dt_{\rho_i} dt_{\rho_i+1} \quad (6)$$

where $\bar{x} = 1 - x$ and $f_{t_j}(t_j)$ in (6) is the pdf of t_j , which can be either $f_{\tau_{id}}(\cdot)$ or $f_{\tau_{ac}}(\cdot)$ depending on whether the underlying interval is idle or active one, respectively.

In this expression, we have averaged over the possible distribution of the time interval vector \vec{t}^k whose elements t_j^i vary according to the exact state transition instant within the corresponding data fragment. The quantity in (5) accounts for $2^{\bar{K}}$ different possible sensing outcomes in \bar{K} fragments. Moreover, the term $\sum_{j_3 \in \bar{\Phi}_k^0} T_{j_3}(\vec{t}^k)$ represents the corresponding achieved throughput for the underlying pattern \mathcal{S}_i and sensing outcomes. Note that the data phase must start with the idle state, which explains the factor $\mathcal{P}(\mathcal{H}_0)$ in this expression. Moreover, the first channel transition must be from idle to active, i.e., $f_{t_1}(t_1) = f_{\tau_{id}}(t_1)$. In general, if j is odd, then $f_{t_j}(t_j) = f_{\tau_{id}}(t_j)$; otherwise, $f_{t_j}(t_j) = f_{\tau_{ac}}(t_j)$.

We now interpret the term in (5) in details. For particular sensing outcomes in all fragments, we have defined two subsets, namely a set of fragments Φ_k^0 where the sensing indicates an available channel and the complement set of fragments Φ_k^1 where the sensing indicates a busy channel. Moreover, we have defined the set $\bar{\Phi}_k^0$ whose elements are indices of fragments each of which is the next fragment of one corresponding fragment in Φ_k^0 (e.g., if $\Phi_k^0 = \{1, 3\}$ then $\bar{\Phi}_k^0 = \{2, 4\}$). We need the set $\bar{\Phi}_k^0$ since only fragments in this set involve data transmissions and, therefore, contribute to the overall network throughput. In (5), the first two products

TABLE I
DETERMINATION OF \mathcal{P}_j AND T_j FOR FRAGMENT $j \in \Phi_k^0$

\mathcal{P}_j	T_j	Conditions
$\overline{\mathcal{P}}_f^{00}$	T^{00}	$(j \in \mathcal{S}^{00}) \cap \{(j-1) \in \Phi_k^0 \cup (j-1=1)\}$
$\overline{\mathcal{P}}_{f,h}^{00}$	0	$(j \in \mathcal{S}^{00}) \cap (j-1) \in \Phi_k^1$
$\overline{\mathcal{P}}_f^{10}$	T^{10}	$(j \in \mathcal{S}^{10}) \cap \{(j-1) \in \Phi_k^0 \cup (j-1=1)\}$
$\overline{\mathcal{P}}_{f,h}^{10}$	0	$(j \in \mathcal{S}^{10}) \cap (j-1) \in \Phi_k^1$
$\overline{\mathcal{P}}_d^{11}$	T^{11}	$(j \in \mathcal{S}^{11}) \cap \{(j-1) \in \Phi_k^0 \cup (j-1=1)\}$
$\overline{\mathcal{P}}_{d,h}^{11}$	0	$(j \in \mathcal{S}^{11}) \cap (j-1) \in \Phi_k^1$
$\overline{\mathcal{P}}_d^{01}$	T^{01}	$(j \in \mathcal{S}^{01}) \cap \{(j-1) \in \Phi_k^0 \cup (j-1=1)\}$
$\overline{\mathcal{P}}_{d,h}^{01}$	0	$(j \in \mathcal{S}^{01}) \cap (j-1) \in \Phi_k^1$

represent the probability of sensing outcomes for all fragments in the k -th sensing outcome.

In the following, we present the derivations of \mathcal{P}_j and T_j . Let \mathcal{P}_d^{11} , \mathcal{P}_d^{01} , \mathcal{P}_f^{00} , and \mathcal{P}_f^{10} denote the probabilities of detection and false alarm for the following channel state transition events \mathcal{H}_{11} , \mathcal{H}_{01} , \mathcal{H}_{00} and \mathcal{H}_{10} using FD sensing, respectively. Similarly, we denote $\mathcal{P}_{d,h}^{11}$ and $\mathcal{P}_{d,h}^{01}$, $\mathcal{P}_{f,h}^{00}$ and $\mathcal{P}_{f,h}^{10}$ as the probabilities of detection and false alarm for events \mathcal{H}_{11} , \mathcal{H}_{01} , \mathcal{H}_{00} and \mathcal{H}_{10} using HD sensing, respectively. Derivations of the probabilities of detection and false alarm for all events and all sensing schemes are given in Appendix A. Let T^{00} , T^{10} , T^{01} and T^{11} denote the number of bits per Hz under the state transition events \mathcal{H}_{00} , \mathcal{H}_{10} , \mathcal{H}_{01} and \mathcal{H}_{11} , respectively. These quantities are derived in Appendix B.

For particular fragment $j \in \Phi_k^0$, the quantities \mathcal{P}_j and T_j are given in Table I where \cap and \cup denote AND and OR operations, respectively. For example, in the first line, if the sensing outcome indicates an available channel in fragment $j-1$ ($(j-1) \in \Phi_k^0$) or fragment $j-1$ is the first one in the data access phase then the SU will perform concurrent sensing and transmission in fragment j . Moreover, fragment j belongs to the set \mathcal{S}^{00} ; therefore, we have $\mathcal{P}_j = \overline{\mathcal{P}}_f^{00}$ and $T_j = T^{00}$. Similarly, we can interpret the results for \mathcal{P}_j and T_j in other cases. For fragment $j \in \Phi_k^1$, to calculate the quantities \mathcal{P}_j , we use the results in the first column of Table I but we have to change all items to \mathcal{P}_x^{kl} ($k, l \in \{0, 1\}$, x represents f , d , fh , and dh). Note that all the quantities depends on time instant t when the PU changes its state. For example, at the time point t_j corresponding to fragment l_j , $t = \sum_{k=1}^j t_k - [T_{\text{ove}}(i_0) + (l_j - 1)T]$. We have omitted this dependence on t in all notations for brevity (details can be found in Appendices A and B).

In summary, we have derived $\mathcal{T}^{i_0}\{\mathcal{S}_i\}$, which can be substituted into (4) to obtain \mathcal{T}^{i_0} . Finally, applying the result of \mathcal{T}^{i_0} to (1), we can calculate the secondary network throughput \mathcal{NT} .

V. CONFIGURATION OF MAC PROTOCOL FOR THROUGHPUT MAXIMIZATION

A. Problem Formulation

We are interested in determining optimal configuration of the proposed MAC protocol to achieve the maximum throughput while satisfactorily protecting the PU. Specifically, let $\mathcal{NT}(T, W, P_s)$ denote the normalized secondary throughput, which is the function of fragment time T , contention window W , and SU's transmit power P_s . Suppose that the PU requires that the average detection probability achieved at fragment i be at least $\overline{\mathcal{P}}_{d,i}$. Then, the throughput maximization problem can be stated as follows:

$$\begin{aligned} & \max_{T, W, P_s} \mathcal{NT}(T, W, P_s) \\ \text{s.t. } & \hat{\mathcal{P}}_{d,i}(\varepsilon^i, T) \geq \overline{\mathcal{P}}_{d,i}, \quad i = 1, 2, \dots, \overline{K} \\ & 0 < T \leq T_{\text{eva}}, \quad 0 < W \leq W_{\text{max}}, \\ & 0 < P_s \leq P_{\text{max}}, \end{aligned} \quad (7)$$

where W_{max} is the maximum contention window, P_{max} is the maximum power for SUs and the fragment time T is upper bounded by T_{eva} . In fact, the first constraint on $\hat{\mathcal{P}}_{d,i}(\varepsilon^i, T)$ implies that the spectrum sensing should be sufficiently reliable to protect the PU where the fragment time (also sensing time) T must be sufficiently large. Moreover, the optimal contention window W should be set to balance between reducing collisions among SUs and limiting protocol overhead. Finally, the SU's transmit power P_s must be appropriately set to achieve good tradeoff between the network throughput and self-interference mitigation in spectrum sensing.

B. Configuration Algorithm for MAC Protocol

Algorithm 1 MAC CONFIGURATION ALGORITHM

```

1: for each value of  $W \in [1, W_{\text{max}}]$  do
2:   for each searched value of  $T \in (0, T_{\text{eva}}]$  do
3:     Find optimal  $P_s^*$  as  $P_s^* = \underset{0 \leq P_s \leq P_{\text{max}}}{\text{argmax}} \mathcal{NT}(T, W, P_s)$ .
4:   end for
5:   The best  $(T^*, P_s^*)$  for each  $W$  is  $(T^*, P_s^*) = \underset{T, P_s^*}{\text{argmax}} \mathcal{NT}(T, W, P_s^*)$ .
6: end for
7: The final solution  $(W^*, T^*, P_s^*)$  is determined as  $(W^*, T^*, P_s^*) = \underset{W, T^*, P_s^*}{\text{argmax}} \mathcal{NT}(W, T^*, P_s^*)$ .
```

We assume the shifted exponential distribution for τ_{ac} and τ_{id} where $\bar{\tau}_{\text{ac}}$ and $\bar{\tau}_{\text{id}}$ are their corresponding average values of the exponential distribution. Specifically, let $f_{\tau_x}(t)$ denote the pdf of τ_x (x represents ac or id as we calculate the pdf of τ_{ac} or τ_{id} , respectively) then

$$f_{\tau_x}(t) = \begin{cases} \frac{1}{\bar{\tau}_x} \exp\left(-\frac{t - T_{\text{min}}^x}{\bar{\tau}_x}\right) & \text{if } t \geq T_{\text{min}}^x \\ 0 & \text{if } t < T_{\text{min}}^x \end{cases} \quad (8)$$

For a given T , we would set the sensing detection threshold ε and SU's transmit power P_s so that the constraint on the average detection probability is met with equality, i.e., $\hat{\mathcal{P}}_d(\varepsilon, T) = \overline{\mathcal{P}}_d$ as in [3], [4]. In addition, the first constraint in (7) now turns to the two constraints for the average probabilities of detection under FD and HD spectrum sensing. First, the average probability of detection under FD sensing can be expressed as

$$\hat{\mathcal{P}}_d = \frac{\mathcal{P}_d^{11} \mathcal{P}(\mathcal{H}_{11}) + \overline{\mathcal{P}}_d^{01} \mathcal{P}(\mathcal{H}_{01})}{\mathcal{P}(\mathcal{H}_{11}) + \mathcal{P}(\mathcal{H}_{01})} \quad (9)$$

where \mathcal{P}_d^{11} is the probability of detection for \mathcal{H}_{11} ; $\overline{\mathcal{P}}_d^{01}$ is the average probability of detection for \mathcal{H}_{01} , which is given as

$$\overline{\mathcal{P}}_d^{01} = \int_{T_{\text{min}}^{\text{id}}}^{T + T_{\text{min}}^{\text{id}}} \mathcal{P}_d^{01}(t) f_{\tau_{\text{id}}}(t | T_{\text{min}}^{\text{id}} \leq t \leq T + T_{\text{min}}^{\text{id}}) dt \quad (10)$$

where $f_{\tau_{\text{id}}}(t | \mathcal{A})$ is the pdf of τ_{id} conditioned on $\mathcal{A} = T_{\text{min}}^{\text{id}} \leq t \leq T + T_{\text{min}}^{\text{id}}$, which is given as

$$f_{\tau_{\text{id}}}(t | \mathcal{A}) = \frac{f_{\tau_x}(t)}{\Pr\{\mathcal{A}\}} = \frac{\frac{1}{\bar{\tau}_{\text{id}}} \exp\left(-\frac{t}{\bar{\tau}_{\text{id}}}\right)}{1 - \exp\left(-\frac{T}{\bar{\tau}_{\text{id}}}\right)}. \quad (11)$$

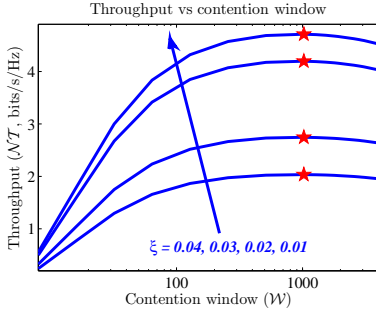


Fig. 3. Normalized throughput versus contention window W for $T = 18ms$, $\bar{\tau}_{id} = 1000ms$, $\bar{\tau}_{ac} = 100ms$, $\bar{K} = 4$ and varying ξ .

Note that \mathcal{P}_d^{11} and $\mathcal{P}_d^{01}(t)$ are derived in Appendix A. Moreover, $\mathcal{P}(\mathcal{H}_{01})$ and $\mathcal{P}(\mathcal{H}_{11})$ are the probabilities of events \mathcal{H}_{01} and \mathcal{H}_{11} , which are given as

$$\mathcal{P}(\mathcal{H}_{01}) = \mathcal{P}(\mathcal{H}_0) \Pr(T_{\min}^{\text{id}} \leq \tau_{id} \leq T + T_{\min}^{\text{id}}) = \mathcal{P}(\mathcal{H}_0) \left[1 - \exp\left(-\frac{T}{\bar{\tau}_{id}}\right) \right] \quad (12)$$

$$\mathcal{P}(\mathcal{H}_{11}) = \mathcal{P}(\mathcal{H}_1) \Pr(\tau_{ac} \geq T + T_{\min}^{\text{ac}}) = \mathcal{P}(\mathcal{H}_1) \exp\left(-\frac{T}{\bar{\tau}_{ac}}\right) \quad (13)$$

The average probability of detection for HD sensing, $\hat{\mathcal{P}}_{d,h}$ can be derived similarly.

We propose an algorithm to determine (T, W, P_s) summarized in Alg. 1. Note that there is a finite number of values for $W \in [1, W_{\max}]$; therefore, we can perform exhaustive search to determine its best value. Moreover, we can use the bisection scheme to determine the optimal value of T . Furthermore, the optimal value of P_s can be determined by a numerical method for given T and W in step 3. Then, we search over all possible choices of T and W to determine the optimal configuration of the parameters (in steps 5 and 7).

C. Half-Duplex MAC Protocol with Periodic Sensing

To demonstrate the potential performance gain of the proposed FD MAC protocol, we also consider an HD MAC protocol. In this HD MAC protocol, we perform the same backoff for channel resolution but we employ periodic HD sensing in each data fragment where the sensing duration is T_S and data transmission duration is $T - T_S$. If the sensing outcome in the sensing stage indicates an available channel then the SU transmit data in the second stage; otherwise, it will keep silent for the remaining time of fragment and wait for the next fragment. Due to the space constraint, throughput analysis for this HD MAC protocol is given in the online technical report [10].

VI. NUMERICAL RESULTS

To obtain numerical results, we take key parameters for the MAC protocol from Table II in [9]. All other parameters are chosen as follows unless stated otherwise: mini-slot is $\sigma = 20\mu s$; sampling frequency is $f_s = 6\text{MHz}$; bandwidth of PU's QPSK signal is 6MHz; $\bar{\mathcal{P}}_d = 0.8$; $T_{\text{eva}} = 40\text{ms}$; $T_{\min}^{\text{ac}} = 40\text{ms}$; $T_{\min}^{\text{id}} = 45\text{ms}$; the SNR of PU signals at SUs $\gamma_P = \frac{P_p}{N_0} = -20\text{dB}$; the self-interference parameters $\zeta = 0.4$ and varying ξ . Without loss of generality, the noise power is normalized to one; hence, the SU transmit power, P_s becomes $P_s = SNR_s$; and $P_{\max} = 25\text{dB}$.

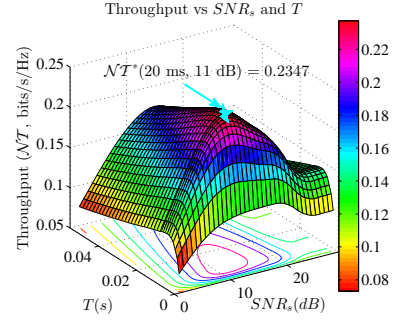


Fig. 4. Normalized throughput versus SU transmit power P_s and length of fragment T for $W = 1024$, $\bar{\tau}_{id} = 200ms$, $n_0 = 40$, $\bar{\tau}_{ac} = 100ms$, $\bar{K} = 4$, $\xi = 0.95$ and $\zeta = 0.6$.

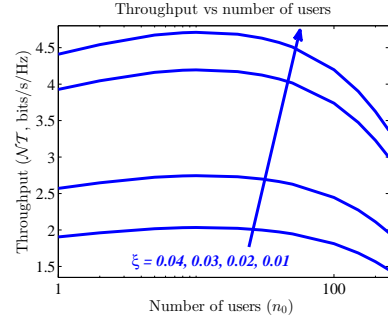


Fig. 5. Normalized throughput versus number of SUs n_0 for $T = 18ms$, $W = 1024$, $\bar{\tau}_{id} = 1000ms$, $\bar{\tau}_{ac} = 100ms$, $\bar{K} = 4$ and varying ξ .

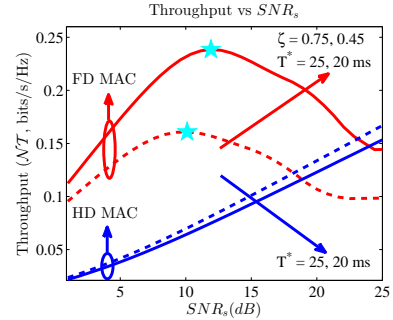


Fig. 6. Normalized throughput versus P_s for $(\bar{\tau}_{id}, \bar{\tau}_{ac}) = (200, 100)$ ms, $n_0 = 40$, $\bar{K} = 4$, $\xi = 0.9$ and $\zeta = \{0.45, 0.75\}$.

We first consider the effect of self-interference on the throughput performance where $\zeta = 0.4$ and ξ is varied in $\xi = \{0.01, 0.02, 0.03, 0.04\}$. Fig. 3 illustrates the variations of the throughput versus contention window W . It can be observed that when ξ decreases (i.e., the self-interference is smaller), the achieved throughput increases. This is because the SU can transmit with higher power while still maintaining the sensing constraint, which leads to throughput improvement. The optimal P_s corresponding to these values of ξ are $P_s = SNR_s = \{25.00, 18.19, 13.56, 10.78\}\text{dB}$ and the optimal contention window is indicated by a star.

Fig. 4 illustrates the throughput performance versus SU transmit power P_s and length of fragment T where $\xi = 0.95$, $\zeta = 0.45$, $T_{\text{eva}} = T_{\min}^{\text{ac}} = T_{\min}^{\text{id}} = 40\text{ms}$, $P_{\max} = 30\text{dB}$. It can be observed that there exists an optimal configuration of SU transmit power $P_s^* = 11\text{dB}$ and fragment time $T^* = 20\text{ms}$ to achieve the maximum throughput $\mathcal{NT}(T^*, P_s^*) = 0.2347$, which is indicated by a star symbol. This demonstrates the sig-

nificance of power allocation to mitigate the self-interference and the optimization of fragment time T to effectively exploit the spectrum opportunity. Fig. 5 illustrates the throughput performance versus number of SUs, n_0 where $\zeta = 0.4$ and ξ is varied in the set $\xi = \{0.01, 0.02, 0.03, 0.04\}$. Again, when ξ decreases (i.e., the self-interference is smaller), the achieved throughput increases. In this figure, the SNR_s corresponding to the considered values of ξ are $P_s = SNR_s = \{25.00, 18.19, 13.56, 10.78\} dB$.

Finally, we compare the throughput of our proposed FD MAC protocol and the HD MAC protocol with periodic sensing in Fig. 6. For fair comparison, we first obtain the optimal configuration of FD MAC protocol, i.e., (T^*, W^*, P_s^*) ($(20ms, 1024, 12dB)$ for $\zeta = 0.45$ and $(25ms, 1024, 10dB)$ for $\zeta = 0.75$), then we use (T^*, W^*) for the HD MAC protocol. Moreover, we optimize sensing time, T_S to maximize the achieved throughput for the HD MAC protocol. We can see that when the self-interference is higher (i.e., ζ increases), the FD MAC protocol requires higher fragment length, T but lower SU transmit power, P_s . For both studied cases of ζ , our proposed FD MAC protocol with power allocation outperforms the HD MAC protocol at the corresponding optimal power levels required by the FD MAC protocol. Moreover, we can observe that our proposed FD MAC protocol can achieve the maximum throughput at the transmit power level less than P_{max} while the HD MAC protocol achieves the maximum throughput at P_{max} since it does not suffer from the self-interference.

VII. CONCLUSION

In this paper, we have proposed the FD MAC protocol for FDCRN that explicitly takes into account the self-interference. Specifically, we have derived the normalized throughput of the proposed MAC protocols and determined their optimal configuration for throughput maximization. Finally, we have presented numerical results to demonstrate the desirable performance of the proposed design.

APPENDIX A

PROBABILITIES OF A FALSE ALARM AND DETECTION

Assume that the transmitted signals from the PU and SU transmitter are circularly symmetric complex Gaussian (CSCG) signals while the noise at the secondary links is independent and identically distributed CSCG $\mathcal{CN}(0, N_0)$ [3]. Under FD sensing, the probability of a false alarm for event \mathcal{H}_{00} can be derived using the similar method as the one in [3], which is given as

$$\mathcal{P}_f^{00} = \mathcal{Q} \left[\left(\frac{\epsilon}{N_0 + I} - 1 \right) \sqrt{f_s T} \right] \quad (14)$$

where $\mathcal{Q}(x) = \int_x^{+\infty} \exp(-t^2/2) dt$; f_s , N_0 , ϵ , I are the sampling frequency, the noise power, the detection threshold and the self-interference, respectively. The probability of detection for event \mathcal{H}_{11} is

$$\mathcal{P}_d^{11} = \mathcal{Q} \left[\left(\frac{\epsilon}{N_0 + I} - \gamma_{PS} - 1 \right) \frac{\sqrt{f_s T}}{\gamma_{PS} + 1} \right] \quad (15)$$

where $\gamma_{PS} = \frac{P_p}{N_0 + I}$ is the signal-to-interference-plus-noise ratio (SINR) of the PU's signal at the SU.

Similarly, we can express \mathcal{P}_f^{10} and \mathcal{P}_d^{01} as follows:

$$\mathcal{P}_f^{10} = \mathcal{Q} \left(\frac{\left(\frac{\epsilon}{N_0 + I} - \frac{t}{T} \gamma_{PS} - 1 \right) \sqrt{f_s T}}{\sqrt{\frac{t}{T} (\gamma_{PS} + 1)^2 + 1 - \frac{t}{T}}} \right) \quad (16)$$

$$\mathcal{P}_d^{01} = \mathcal{Q} \left(\frac{\left(\frac{\epsilon}{N_0 + I} - \frac{T-t}{T} \gamma_{PS} - 1 \right) \sqrt{f_s T}}{\sqrt{\frac{T-t}{T} (\gamma_{PS} + 1)^2 + \frac{t}{T}}} \right) \quad (17)$$

where t is the time instant when the PU changes its state. For HD sensing, the expressions for the probabilities of detection and a false alarm for the corresponding four events are similar to the ones for FD sensing except that the self-interference-plus-noise power $N_0 + I$ becomes noise power N_0 only; hence, γ_{PS} becomes $\gamma_{PS}^h = \frac{P_p}{N_0}$.

APPENDIX B FRAGMENT THROUGHPUT

For \mathcal{H}_{00} , the average throughput T^{00} is

$$T^{00} = T \log_2(1 + \gamma_{S1}) \quad (18)$$

where $\gamma_{S1} = \frac{P_s}{N_0 + I}$ is the SINR of received signal at the SU receiver when the PU is idle. Similarly, we can write T^{10} , T^{01} and T^{11} as follows:

$$T^{10} = [t \log_2(1 + \gamma_{S2}) + (T - t) \log_2(1 + \gamma_{S1})] \quad (19)$$

$$T^{01} = [t \log_2(1 + \gamma_{S1}) + (T - t) \log_2(1 + \gamma_{S2})] \quad (20)$$

$$T^{11} = T \log_2(1 + \gamma_{S2}) \quad (21)$$

where $\gamma_{S2} = \frac{P_s}{N_0 + I + P_p}$ is the SINR of the received signal at the SU receiver when the PU is active, and t is the time instant at which the PU changes its activity state.

REFERENCES

- [1] T. Yucek and H. Arslan, "A survey of spectrum sensing algorithms for cognitive radio applications," *IEE Commun. Surveys and Tutorials*, vol. 11, no. 1, pp. 116–130, 2009.
- [2] C. Cormio and K. R. Chowdhury, "A survey on MAC protocols for cognitive radio networks," *Elsevier Ad Hoc Networks*, vol. 7, no. 7, pp. 1315–1329, Sept. 2009.
- [3] Y. C. Liang, Y. H. Zeng, E. C. Y. Peh, and A. T. Hoang, "Sensing-throughput tradeoff for cognitive radio networks," *IEEE Trans. Wireless Commun.*, vol. 7, no. 4, pp. 1326–1337, April 2008.
- [4] L. T. Tan and L. B. Le, "Distributed MAC protocol for cognitive radio networks: Design, analysis, and optimization," *IEEE Trans. Veh. Technol.*, vol. 60, no. 8, pp. 3990–4003, Oct. 2011.
- [5] L. T. Tan and L. B. Le, "Channel assignment with access contention resolution for cognitive radio networks," *IEEE Trans. Veh. Technol.*, vol. 61, no. 6, pp. 2808–2823, April 2012.
- [6] Y.R. Kondareddy, and P. Agrawal, "Synchronized MAC protocol for multi-hop cognitive radio networks," in *Proc. IEEE ICC'2008*.
- [7] W. Afifi and M. Krunz, "Incorporating self-interference suppression for full-duplex operation in opportunistic spectrum access systems," *IEEE Trans. Wireless Commun.*, vol. 14, no. 4, April 2015.
- [8] M. Duarte, C. Dick, and A. Sabharwal, "Experiment-driven characterization of full-duplex wireless systems," *IEEE Trans. Wireless Commun.*, vol. 11, no. 12, pp. 4296–4307, Dec. 2012.
- [9] G. Bianchi, "Performance analysis of the IEEE 802.11 distributed coordination function," *IEEE J. Sel. Areas Commun.*, vol. 18, no. 3, pp. 535–547, Mar. 2000.
- [10] L. T. Tan and L. B. Le, "Distributed MAC protocol design for full-duplex cognitive radio networks," technical report. Online: <http://www.necphy-lab.com/pub/TanReport.pdf>